Available online at www.sciencedirect.com
ScienceDirect
International Journal of Heat and Mass Transfer 51 (2008) 1955–1961
International Journal of HEAT and MASS TRANSFER
www.elsevier.com/locate/ijhmt

Density maximum effect on buoyancy-driven convection of water in a porous cavity with variable side wall temperatures

P. Kandaswamy *, M. Eswaramurthi

UGC-DRS Centre for Fluid Dynamics, Department of Mathematics, Bharathiar University, Coimbatore 641 046, India

Received 4 April 2007; received in revised form 8 June 2007
Available online 24 August 2007

Abstract

The buoyancy-driven convection in a square cavity filled with water-saturated porous medium is studied numerically. While the right and left side wall temperatures vary linearly from θ_a to θ_o and θ_o to θ_b, respectively with height and θ_o is the mean of θ_a and θ_b, the top and bottom walls of the cavity are thermally insulated. The Brinkman–Forchheimer extended Darcy model is considered to study the effects of density maximum, Grashof numbers, porosity and Darcy numbers on the buoyancy-induced flow and heat transfer. The finite volume method is used to discretize the governing equations, which are solved by Gauss–Seidel and successive over relaxation methods. The temperature distribution and flow fields are presented in the form of streamlines, isotherms and mid-height velocity profiles. It is found that the effect of density maximum is to slow down the natural convection and reduce the average heat transfer. The strength of convection and heat transfer rate become weak due to more flow restriction in the porous medium for small porosity.

Keywords: Natural convection; Porosity; Density maximum

1. Introduction

The problem of fluid flow and heat transfer in porous media are encountered in different applications such as oil recovery, underground water flow, high-performance insulation for building and cryogenic containers particularly in the field of large storage system of agricultural products. The buoyancy-driven convection in a fluid-saturated porous medium is an important study nowadays in devising and designing engineering equipments. The devices include heat exchangers, planar reactors and industrial furnaces which find natural and technical applications of buoyancy-driven convection. The buoyancy driven convection arises in a fluid due to the density variations caused by the temperature differences of the system.

Several studies on buoyancy-driven fluid flow and heat transfer in porous media have been reported for different physical formulation and geometric models with various boundary conditions. The model commonly used consists of a porous cavity with both the vertical walls maintained at constant temperatures or one vertical wall subject to a constant heat flux and the other vertical isothermal wall, while the horizontal walls are adiabatic. The paper studies numerically the buoyancy-driven convection in a porous cavity with linearly varying temperatures. The hot and cold walls are vertical walls while the horizontal walls are adiabatic. Convection in water behaves differently around the temperature region of 4 °C due to the anamolous behavior of density around this temperature and the density of water at both side walls of the cavity varies non-linearly with the temperature. A linear temperature-density relationship has been considered in most of the analytical and numerical studies, presented in the literature on natural convection of water in porous-filled rectangular/square enclosures. The present work is a report of an investigation of the effect of the density extremum of water and varied parameters of the porous medium on heat transfer. Buoyancy forces can induce motion in liquids contained in enclosures with

* Corresponding author. Tel.: +91 422 2426764; fax: +91 422 2422387.
E-mail address: pgkswamy@yahoo.co.in (P. Kandaswamy).

0017-9310/$ - see front matter © 2007 Elsevier Ltd. All rights reserved.
doi:10.1016/j.ijheatmasstransfer.2007.06.031

differentially heated side walls. The flows associated with this mechanism have been extensively studied by many authors. A few closely related studies needed to follow the present work only are reviewed in this section.

Poulikakos [1] investigated the natural convection in a fluid-saturated porous layer differentially heated in the horizontal direction. The study shows that the bicellular flow field is the result of the existence of the density maximum. Ettefagh et al. [2] analyzed the importance of non-Darcian effects in open-ended cavities filled with a fluid-saturated porous medium, using Brinkman-extended Darcy, Forchheimer-extended Darcy and generalized flow models. Their results show the significance of both the Forchheimer and the Brinkman modifications on the predictions of buoyancy-induced flow and heat transfer.

Nithiarasu et al. [3] investigated the natural convective flow and associated heat transfer in a fluid-saturated porous medium using the generalized approach. It is shown that a highly convective regime with strong channeling near the walls and higher heat transfer rates to occur for higher Darcy, Rayleigh and Biot numbers. Das and Sahoo [4] studied the effect of Darcy, Rayleigh and heat generation parameters on natural convection in a porous square enclosure, using the Brinkman-extended Darcy model. It is reported that the peak temperature occurs at the top central part and weaker velocity prevails near the vertical walls of the enclosure due to the heat generation parameter alone.

Kandaswamy and Kumar [5] studied numerically the effect of a magnetic field on the buoyancy-driven flow of water inside a square cavity with differentially heated side walls. Their report reveals that the average Nusselt number decreases with an increase in the Hartmann number. Sundaravadivelu and Kandaswamy [6] used a fourth order polynomial approximation for the temperature-density relation to study the buoyancy-driven non-linear convection in a square cavity. It is reported that the heat transfer rate depends nonlinearly on the temperature gradient. Zheng et al. [7] studied convection in a square cavity filled with an anisotropic porous medium saturated with water near 4 °C. It reveals that the Nusselt number is to be maximum when the maximum permeability is in the vertical direction for the case where the principal axes are parallel and perpendicular to the gravity vector. Khanafer and Vafai [8] carried out a study on double diffusive mixed convection in a lid-driven enclosure filled with a non-Darcy fluid saturated porous medium. This study reveals that the buoyancy ratio, the Darcy and Lewis numbers have profound effects on the double diffusive phenomenon.

Osorio et al. [9] reviewed experimental and numerical results of the natural convection of water in an inclined square cavity at temperatures near its maximum density. Saeid and Pop [10] conducted a numerical study on the effects of maximum density on natural convection from a discrete heater in a cavity filled with porous medium. They have reported that the existence of buoyancy force reversals resulting from the maximum density effect results in a reduction of the convective flow and average Nusselt number. Hossain and Rees [11] investigated the effect of the density maximum of water on natural convection in a rectangular enclosure having isothermal walls with heat generation. Their study shows the flow and temperature fields to depend very strongly on the internal heat generation parameter and the differences in temperatures at the side walls.

Tanmay et al. [12] studied the effects of various thermal boundary conditions on natural convection in a square cavity filled with a porous medium. In their work, Darcy–Forchheimer model is used to simulate the momentum transfer in the porous medium. They have reported that the non-uniform heating exhibits greater heat transfer rate at the center of the bottom wall than that with uniform heating case for all Rayleigh number regimes. It reveals that the rate of heat transfer increases when the tilting angle of the cavity takes lower negative values and with increase in the internal sources. Kandaswamy et al. [13] estimates through a numerical investigation on transient natural convection of cold water around its density maximum in a square cavity that the average heat transfer rate behaves non-linearly as a function of Grashof numbers. Sathiyamoorthy et al. [14] studied the influence of linearly heated vertical wall(s) and uniformly heated bottom wall on flow and heat transfer characteristics due to natural convection within a square cavity filled with porous medium. In the case of linearly heated side walls, they found the presence of symmetric strong secondary circulations to enhance the local mixing process in the lower half of the cavity for low Prandtl number.

Kaviany [15] describes the effect of porosity on the convective flow of a fluid in porous media. Nield and Bejan [16] provide a comprehensive literature survey on natural convection in porous media. Vafai [17] gives a deep insight into convective heat transfer in porous media. The limitations of most of the existing studies in a porous cavity are (i) using Darcy flow model and (ii) using linear density-temperature relations. The density of water reaches a maximum value at a specific temperature and decreases when deviating from that temperature. As a result, the Boussinesq approximation is not applicable to such fluids. The present study uses the Brinkman–Forchheimer extended Darcy model to investigate the effect of water density maximum, Grashof number, Darcy number and porosity on heat transfer inside a square cavity filled with a water saturated porous medium.

2. Mathematical formulation

Consider a two-dimensional square cavity of side L with water saturated porous medium as shown in Fig. 1. The vertical walls are maintained at two different varying temperatures. The lower end of right sidewall of the cavity is maintained at a constant temperature θ_a (=273 K). The upper end of left sidewall of the cavity is maintained at temperature $\theta_b(>\theta_a)$. The temperature θ_o is the average of

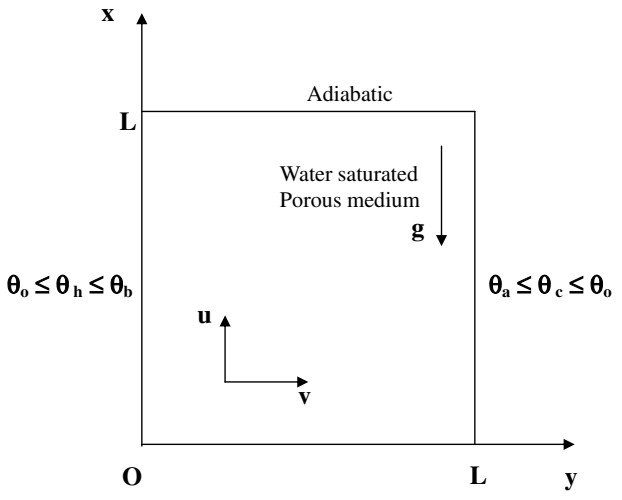

Fig. 1. Physical configuration.

the temperatures θ_a and θ_b. The right wall temperature is varying linearly from the bottom (θ_a) to the top (θ_o). The left wall temperature is varying linearly from the bottom (θ_o) to the top (θ_b). The horizontal walls are adiabatic. The gravity acts in the downward direction. The velocity components u and v are taken in the x and y directions, respectively.

The porous medium is assumed to be isotropic, homogeneous and in thermodynamic equilibrium with the fluid. Also,it is assumed that the solid matrix and the fluid are in local thermodynamic equilibrium. The flow in the cavity is assumed to be two-dimensional, laminar and incompressible with negligible viscous dissipation. The specific heat ratio (σ) is assumed to be one. The thermophysical properties of the fluid are assumed to be constant except the density variation in the buoyancy force, which follows the relation, as described by Kandaswamy and Kumar [5] and Sundaravadivelu and Kandaswamy [6], $\rho = \rho_o[1-\sum_{i=1}^{4}(-1)^i\beta_i(\theta-\theta_c)^i]$, where ρ_0 is the density of water at θ_c, $\beta_1 = 6.8143\times10^{-5}$, $\beta_2 = 9.9901\times10^{-6}$, $\beta_3 = 2.7217\times10^{-7}$ and $\beta_4 = 6.7252\times10^{-9}$.

The system of equations governing the two-dimensional motion described above is

$$\frac{\partial u}{\partial x}+\frac{\partial v}{\partial y}=0 \tag{1}$$

$$\frac{1}{\epsilon}\frac{\partial u}{\partial t}+\frac{1}{\epsilon^2}\left[u\frac{\partial u}{\partial x}+v\frac{\partial u}{\partial y}\right] = -\frac{1}{\rho_o}\frac{\partial p}{\partial x}+\frac{v}{\epsilon}\left[\frac{\partial^2 u}{\partial x^2}+\frac{\partial^2 u}{\partial y^2}\right] - \frac{v}{K}u-\frac{1.75}{\sqrt{150}\epsilon^{3/2}}\frac{u\sqrt{u^2+v^2}}{\sqrt{K}} - \frac{\rho}{\rho_o}g \tag{2}$$

$$\frac{1}{\epsilon}\frac{\partial v}{\partial t}+\frac{1}{\epsilon^2}\left[u\frac{\partial v}{\partial x}+v\frac{\partial v}{\partial y}\right] = -\frac{1}{\rho_o}\frac{\partial p}{\partial y}+\frac{v}{\epsilon}\left[\frac{\partial^2 v}{\partial x^2}+\frac{\partial^2 v}{\partial y^2}\right] - \frac{v}{K}v-\frac{1.75}{\sqrt{150}\epsilon^{3/2}}\frac{v\sqrt{u^2+v^2}}{\sqrt{K}} \tag{3}$$

$$\sigma\frac{\partial\theta}{\partial t}+u\frac{\partial\theta}{\partial x}+v\frac{\partial\theta}{\partial y}=\alpha\left[\frac{\partial^2\theta}{\partial x^2}+\frac{\partial^2\theta}{\partial y^2}\right] \tag{4}$$

where θ is the fluid temperature, K is the permeability of the porous medium, ρ is the fluid density, p is the fluid pressure, α is the effective thermal diffusivity, ϵ is the porosity, v is the kinematic viscosity of the fluid, t is time and ω is the vorticity function.

The appropriate initial and boundary conditions are

$$t=0: \quad u=v=0, \quad \theta=\theta_c, \quad 0\leqslant x\leqslant L, \quad 0\leqslant y\leqslant L, \tag{5}$$

$$t>0: \quad u=v=0, \quad \frac{\partial\theta}{\partial x}=0, \quad x=0\&L, \tag{6}$$

$$u=v=0, \quad \theta=(\theta_b-\theta_o)\left(\frac{x}{L}\right)+\theta_o, \quad y=0, \tag{7}$$

$$u=v=0, \quad \theta=(\theta_o-\theta_a)\left(\frac{x}{L}\right)+\theta_a, \quad y=L. \tag{8}$$

The following non-dimensional variables are used

$$(X,Y)=\frac{(x,y)}{L}, \quad (U,V)=\frac{(u,v)}{v/L}, \quad \tau=\frac{t}{L^2/v}, \quad \Psi=\frac{\psi}{v}, \quad \zeta=\frac{\omega}{v/L^2} \text{ and } T=\frac{\theta-\theta_a}{\theta_b-\theta_a}. \tag{9}$$

The governing equations in non-dimensional form reduce to the vorticity-stream function formulation as follows

$$\frac{1}{\epsilon}\frac{\partial\zeta}{\partial\tau}+\frac{1}{\epsilon^2}\left[\frac{\partial\Psi}{\partial Y}\frac{\partial\zeta}{\partial X}-\frac{\partial\Psi}{\partial X}\frac{\partial\zeta}{\partial Y}\right] = \frac{1}{\epsilon}\nabla^2\zeta-\frac{1}{Da}\zeta-\frac{F_c\zeta}{\sqrt{Da}} - \frac{F_c}{\sqrt{Da}|\mathbf{v}|}\left[\frac{\partial\Psi}{\partial Y}\frac{\partial|\mathbf{v}|}{\partial Y}+\frac{\partial\Psi}{\partial X}\frac{\partial|\mathbf{v}|}{\partial X}\right] - \sum_{i=1}^{4} i(-1)^i Gr_i T^{(i-1)}\frac{\partial T}{\partial Y} \tag{10}$$

$$\nabla^2\Psi=-\zeta \tag{11}$$

$$U=\frac{\partial\Psi}{\partial Y}, \quad V=-\frac{\partial\Psi}{\partial X} \text{ and } \zeta=\frac{\partial V}{\partial X}-\frac{\partial U}{\partial Y}. \tag{12}$$

$$\frac{\partial T}{\partial\tau}+\frac{\partial\Psi}{\partial Y}\frac{\partial T}{\partial X}-\frac{\partial\Psi}{\partial X}\frac{\partial T}{\partial Y}=\frac{1}{Pr}\nabla^2 T$$

$$\text{where } F_c=\frac{1.75|\mathbf{V}|}{\sqrt{150}\times\epsilon^{\frac{3}{2}}} \text{ and } |\mathbf{V}|=\sqrt{\left(\frac{\partial\Psi}{\partial X}\right)^2+\left(\frac{\partial\Psi}{\partial Y}\right)^2}. \tag{13}$$

The initial and boundary conditions in dimensionless form are

$$\tau=0: \quad U=V=0, \quad \zeta=T=0, \quad 0\leqslant X\leqslant 1, \quad 0\leqslant Y\leqslant 1, \tag{14}$$

$$\tau > 0: \quad U = V = 0, \quad \Psi = \frac{\partial \Psi}{\partial Y} = 0, \quad \frac{\partial T}{\partial X} = 0,$$
$$X = 0\&1, \quad 0 \leqslant Y \leqslant 1 \tag{15}$$

$$U = V = 0, \quad \Psi = \frac{\partial \Psi}{\partial X} = 0, \quad T = \frac{1}{2}(1+X), \quad Y = 0,$$
$$0 \leqslant X \leqslant 1 \tag{16}$$

$$U = V = 0, \quad \Psi = \frac{\partial \Psi}{\partial X} = 0, \quad T = \frac{1}{2}(X), \quad Y = 1,$$
$$0 \leqslant X \leqslant 1. \tag{17}$$

where ζ is the vorticity, Ψ is the stream function, τ is the non-dimensional time.

The non-dimensional parameters that appear in the equations are $Da = K/L^2$, the Darcy number, $Gr_i = g\beta_i(\theta_h - \theta_c)^i L^3/\nu^2, i = 1,2,3,4$, the Grashof numbers and $Pr = \nu/\alpha = 13.67$, the Prandtl number. The local Nusselt number, a measure for heat transfer across the hot wall, is defined by $Nu = \partial T/\partial Y|_{Y=0}$ and the average Nusselt number is given by $\overline{Nu} = \int_0^1 Nu\,dX$.

3. The method of solution

The non-dimensional governing equations are discretized using finite volume method to form a system of algebraic equations as in Patankar [18]. Gauss–Seidel method is used to solve the system of equations for the energy and vorticity whereas successive over relaxation (SOR) method is used to solve equations for the stream function. Different mesh sizes from 21×21 to 101×101 are used to carry out the study. It is clear from the grid independence test as shown in Fig. 2 that a 41×41 uniform grid is enough to investigate the problem. Thus, after calculating the temperature and vorticity values at an advance point in time $\tau = (n+1)d\tau$ and using their respective solution given at $\tau = (n)d\tau$ ($n = 0$ corresponds to the initial condition), the stream function is solved for its solution at this advanced time step. The time step $d\tau$ is taken to be 10^{-5}.

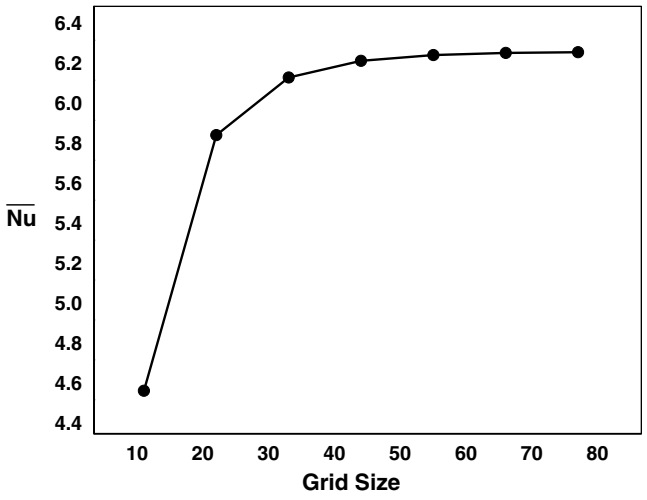

Fig. 2. Average Nusselt number for different grid system.

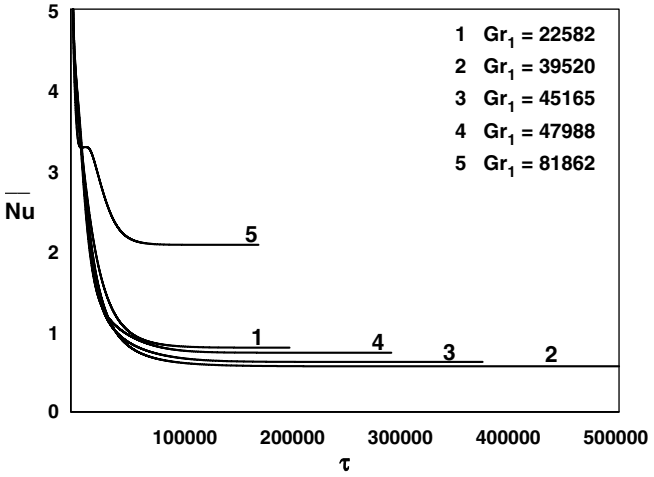

Fig. 3. Time history for different Grashof numbers with $Da = 0.001$ and $\epsilon = 0.4$.

The boundary conditions for ζ are obtained from the relation as described by Rudraiah et al. [19]

$$\zeta = \frac{\Psi_{i,2} - 8\Psi_{i,1}}{2 \times h^2} \tag{18}$$

where 'i' denotes spacial interval in the vertical direction and 'h' denotes the spacial interval in the direction normal to the boundary. The velocity components are obtained from the resulting stream function values. The sequence beginning with the solution of the energy equation is applied repeatedly until the desired accuracy of results are obtained. The convergence criterion used for the field variables $\phi(=T,\zeta,\Psi)$ is $|\frac{\phi_{(n+1)}(i,j) - \phi_{(n)}(i,j)}{\phi_{(n+1)}(i,j)}| \leqslant 10^{-6}$.

Fig. 3 shows the time history of average Nusselt number for different Grashof numbers. The average heat transfer rate decreases as time evolves and attains a constant value, indicating that the steady-state condition prevails. The time scale required to achieve steady-state condition depends on the temperature of density maximum of water which causes formation of dual cell pattern. In the case of single cell pattern, the time taken for convergence is shorter, whereas it is longer in the case of dual cells formation.

4. Results and discussion

Buoyancy-driven convective flow of water in a square cavity filled with water-saturated porous medium is studied numerically around the region of its density maximum. Both the hot and cold wall temperatures vary linearly with height. The computations were carried out for various porosities, Darcy numbers and Grashof numbers. The results are presented as streamlines and isotherms. The rate of heat transfer in the cavity is measured in terms of the average Nusselt number.

Fig. 3 exhibits the time history of average Nusselt number for porosity $\epsilon = 0.4$, $Da = 10^{-3}$ and different Grashof numbers. The average heat transfer rate decreases as time

evolves and attains a constant value, indicating that the steady-state condition prevails. It is clear that higher heat transfer rate is achieved for large Grashof numbers. Figs. 4–8 show the fluid motion and resulting temperature distribution for different Grashof numbers with porosity $\epsilon = 0.4$ and Darcy number $Da = 10^{-3}$. When the hot wall is maintained at the temperature where $Gr_1 = 22{,}582$, the flow pattern consists of a single major cell rotating in the counter clockwise direction as seen in Fig. 4. The temperature distribution inside the cavity is nearly of conduction type. As the density of water near right wall is less than the density of water near left wall, the fluid raises along the right wall and descends along the left wall.

When the hot wall temperature is increased to the temperature for $Gr_1 = 36{,}697$, a secondary vortex rotating in the clockwise direction appears at the top left corner of the cavity near the hot wall, suppressing the primary eddy downwards as seen in Fig. 5. This is because of the anom-

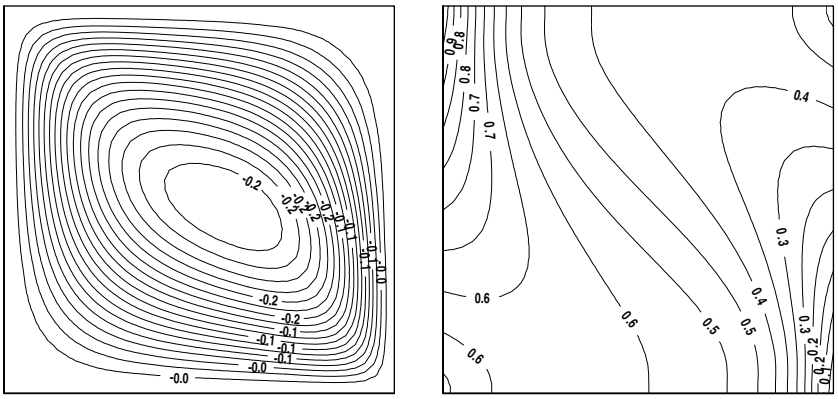

Fig. 4. Stream lines and isotherms for $Gr_1 = 22{,}582$, $\epsilon = 0.4$ and $Da = 0.001$.

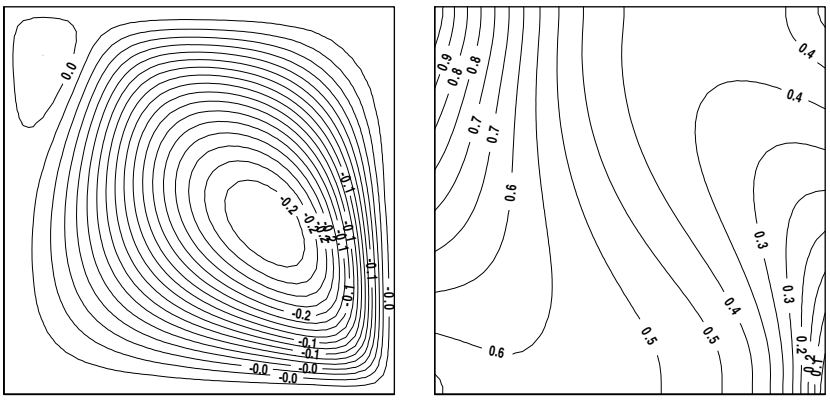

Fig. 5. Stream lines and isotherms for $Gr_1 = 36{,}697$, $\epsilon = 0.4$ and $Da = 0.001$.

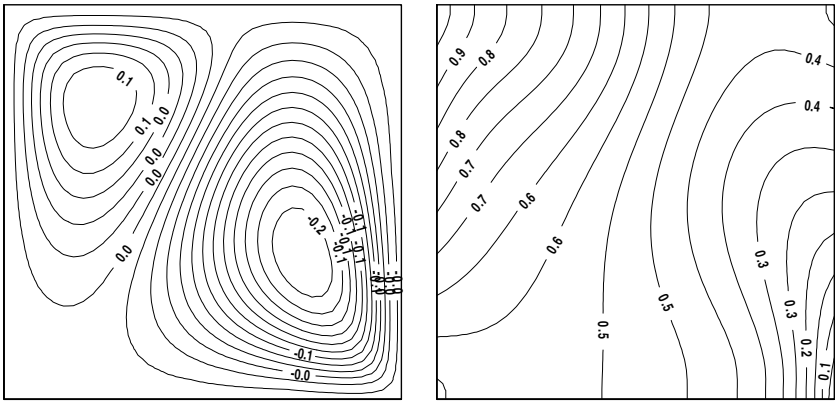

Fig. 6. Stream lines and isotherms for $Gr_1 = 42{,}342$, $\epsilon = 0.4$ and $Da = 0.001$.

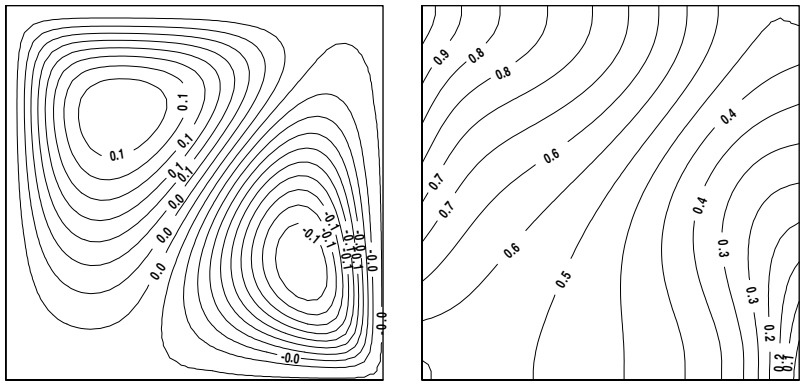

Fig. 7. Stream lines and isotherms for $Gr_1 = 45{,}165$, $\epsilon = 0.4$ and $Da = 0.001$.

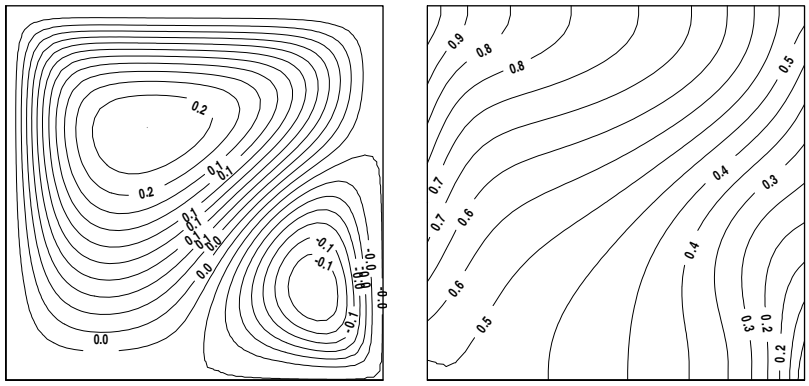

Fig. 8. Stream lines and isotherms for $Gr_1 = 50{,}811$, $\epsilon = 0.4$ and $Da = 0.001$.

alous density behavior of water near 4 °C, which exists away from the left wall. As such, the fluid falls along the plan of density maximum of water, leading to the formation of secondary vertex. The corresponding isotherms get distorted slightly near the upper left corner. Figs. 6 and 7 are presented to show the streamlines and the isotherm patterns for the hot wall temperatures with $Gr_1 = 42{,}342$ and $Gr_1 = 45{,}165$, respectively. In these cases, the secondary eddy gets strengthened suppressing the primary eddy further toward right wall. As the density maximum region moves further towards the right wall in this case, the secondary eddy gets strengthened further. The corresponding isotherms get distorted largely as seen in Fig. 6.

Fig. 7 shows that the secondary cell grows in size along left wall, suppressing the primary eddy towards the right wall for hot wall temperature with $Gr_1 = 45{,}165$. In this case, the density maximum of water exists along the vertical direction in the middle of the cavity. So, the fluid falls in the middle of the cavity and raises along the two vertical walls where the density is less and the bicellular pattern in flow field is noticed for the Grashof number of 45,165 as seen in Fig. 7. This causes reduction in convection heat transfer rate. As the flow rises along the hot wall as well as the cold wall and falls along the plane of maximum density inside the cavity, convective heat transfer rate is reduced to its minimum level at $Gr_1 = 45{,}165$. This unique phenomenon is due to the effect of the density maximum of water near 4 °C as seen in Fig. 7. The streamlines are distorted largely for further increase in temperature at the top of the cavity.

For hot wall temperature with $Gr_1 = 50{,}811$, the clockwise rotating secondary cell spreads to cover major part of the cavity, pushing the counter clockwise rotating primary eddy close to right bottom corner of the cold wall as seen in Fig. 8. The maximum density plane moves further close to cold wall. This results in improving convective heat transfer rate further. As the temperature at top corner of the hot wall increases, the heat transfer rate increases. Fig. 8 shows the streamlines and isotherms for the Grashof number $Gr_1 = 50{,}811$. The corresponding isotherms are almost parallel. Fig. 8 shows that the buoyancy-driven convection dominates in the cavity. The average heat transfer rate improves in this case.

Fig. 9 shows how porosity of the medium affects the average heat transfer rate. As the porosity increases, the heat transfer rate also increases. The higher porosity leads to higher heat transfer rate. This is because of the fluid motion at higher velocity due to larger porosity. Fig. 9 also reveals that the rate of heat transfer is rapid with increase in the porosity. This is because of the vigorous fluid motion inside the cavity. Fig. 10 shows the effect of Darcy numbers

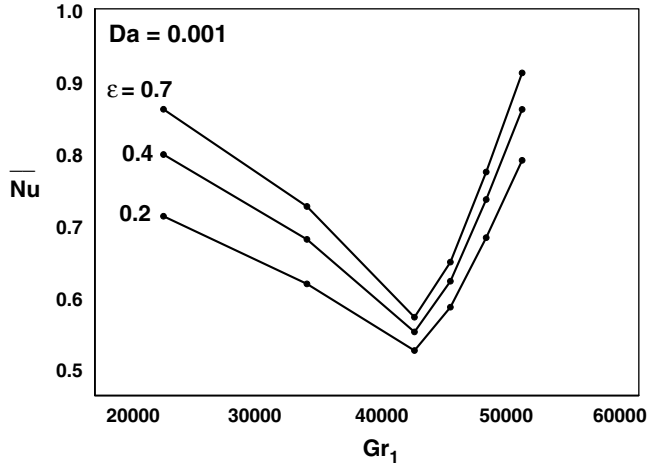

Fig. 9. Average Nusselt number for different Grashof numbers and porosities with $Da = 0.001$.

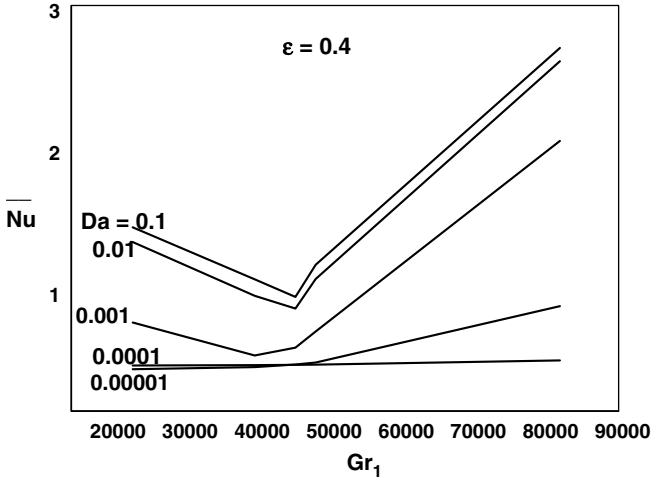

Fig. 10. Average Nusselt number for different Grashof numbers and Darcy numbers with $\epsilon = 0.4$.

on the average heat transfer rate for different Grashof numbers and the porosity $\epsilon = 0.4$. It is observed that the increase in Darcy number enhances the average heat transfer rate. When the Darcy number is very small, the heat transfer takes place by the mode of conduction. The convective heat transfer rate goes down as the Darcy number decreases. The Darcy number, which depends on the permeability of porous medium, leaves strong effects on convection in a porous-filled cavity. The motion of the fluid particle is higher for higher value of Darcy number and the flow is restricted largely in the case of very low value of Darcy numbers.

A clear observation made is that vigorous buoyancy force results inside the cavity, which in turn drives the fluid motion at a high velocity for high Grashof numbers and porosity. But a smaller Darcy number reduces the heat transfer rate. Fig. 3 characterizes the fluid flow and heat transfer in rectangular cavity problems. It brings about an understanding of the time scale required to achieve steady-state condition, determining whether there is an oscillatory or a monotonic approach to the steady-state.

References

[1] D. Poulikakos, Maximum density effects on natural convection in a porous layer differently heated in the horizontal direction, Int. J. Heat Mass Transfer 27 (1984) 2067–2075.
[2] J. Ettefagh, K. Vafai, S.J. Kim, Non-Darcian effects in open-ended cavities filled with a porous medium, J. Heat Mass Transfer 113 (1991) 747–756.
[3] P. Nithiarasu, K.N. Seetharamu, T. Sundararajan, Numerical investigation of buoyancy-driven flow in a fluid-saturated non-Darcy porous medium, Int. J. Heat Mass Transfer. 42 (1999) 205–1215.
[4] S. Das, R.K. Sahoo, Effect of Darcy fluid Rayleigh and heat generation parameters on natural convection in a porous square enclosures: a Brinkman-extended Darcy model, Int. Commun. Heat Mass Transfer 26 (1999) 569–578.
[5] P. Kandaswamy, K. Kumar, Buoyancy-driven nonlinear convection in a square cavity in the presence of a magnetic field, Acta Mech. 136 (1999) 29–39.
[6] K. Sundaravadivelu, P. Kandaswamy, Double diffusive nonlinear convection in a square cavity, Fluid Dyn. Res. 27 (2000) 291–303.
[7] W. Zheng, L. Robillard, P. Vasseur, Convection in a square cavity filled with an anisotropic porous medium saturated with water near 4 °C, Int. J. Heat Mass Transfer 44 (2001) 3463–4370.
[8] K. Khanafer, K. Vafai, Double-diffusive mixed convection in a lid-driven enclosure filled with a fluid-saturated porous medium, Numer. Heat Transfer Part A 42 (2002) 465–486.
[9] A. Osorio, R. Avila, J. Cervantes, On the natural convection of water near its density inversion in a inclined square cavity, Int. J. Heat Mass Transfer 47 (2004) 4491–4495.
[10] N.H. Saeid, I. Pop, Maximum density effects on natural convection from a discrete heater in a cavity filled with a porous medium, Acta Mech. 171 (2004) 203–212.
[11] M.A. Hossain, M.A. Rees, Natural convection flow of water near its density maximum in a rectangular enclosure having isotherm walls with heat generation, Heat Mass Transfer 41 (2005) 367–374.
[12] Tanmay Basak, S. Roy, T. Paul, I. Pop, Natural convection in a porous cavity filled with porous medium: effects of various thermal boundary conditions, Int. J. Heat Mass Transfer 49 (2006) 1430–1441.
[13] P. Kandaswamy, S. Sivasankaran, N. Nithiyadevi, Buoyancy-driven convection of water near its density maximum with partially active vertical walls, Int. J. Heat Mass Transfer 50 (2007) 942–948.
[14] M. Sathiyamoorthy, Tanmay Basak, S. Roy, I. Pop, Steady natural convection flow in a square cavity filled with a porous medium for linearly heated side wall(s), Int. J. Heat Mass Transfer 50 (2007) 1892–1901.
[15] S. Kaviany, Principles of Heat Transfer in Porous Media, Springer-Verlag, New York, 1995.
[16] D.A. Nield, A. Bejan, Convection in Porous Media, Springer Verlag, New York, 1999.
[17] K. Vafai, Handbook of porous media, second ed., Marcel Dekker Inc, 2005.
[18] S.V. Patankar, Numerical Heat Transfer and Fluid Flow, Hemisphere Publishing Corporation, Washington, 1980.
[19] N. Rudraiah, R.M. Barron, M. Venkatachalappa, C.K. Subbaraya, Effect of a magnetic field on free convection in a rectangular enclosure, Int. J. Eng. Sci. 338 (1995) 568–577.